Object Detection, Classification and Localization by Infrastructural Stereo Cameras

Christian Hofmann, Florian Particke, Markus Hiller and Jörn Thielecke
Department of Electrical, Electronic and Communication Engineering, Information Technology,
Friedrich-Alexander-Universitat Erlangen-Nurnberg, Am Wolfsmantel 33, Erlangen, Germany

Keywords: Object Detection, Infrastructural Cameras, Stereo Vision, Deep Learning, Autonomous Driving, Robotics.

Abstract: In the future, autonomously driving vehicles have to navigate in challenging environments. In some situations, their perception capabilities are not able to generate a reliable overview of the environment, by reason of occlusions. In this contribution, an infrastructural stereo camera system for environment perception is proposed. Similar existing systems only detect moving objects by background subtraction algorithms and monocular cameras. In contrast, the proposed approach fuses three different algorithms for object detection and classification and uses stereo vision for object localization. The algorithmic concept is composed of a background subtraction algorithm based on Gaussian Mixture Models, the convolutional neural network ”You only look once” as well as a novel algorithm for detecting salient objects in depth maps. The combination of these complementary object detection principles allows the reliable detection of dynamic as well as static objects. An algorithm for fusing the results of the three object detection methods based on bounding boxes is introduced. The proposed fusion algorithm for bounding boxes improves the detection results and provides an information fusion. We evaluate the proposed concept on real word data. The object detection, classification and localization in the real world scenario is investigated and discussed.

1 INTRODUCTION

State-of-the-art navigation of autonomous vehicles is widely based on maps of static environments. In addition, the vehicle’s own environment perception capabilities are used for navigating. Outdated static environment maps and a perception with a very small field of view lead to challenging navigation situations. An example is an autonomous car in a parking garage, where also pedestrians move. In this environment the autonomous car is not able to detect and localize occluded objects like pedestrians and other obstacles. Besides the difficult navigation, this limited environment perception of the car results in dangerous situations for the pedestrians. To overcome such problematic situations, we propose an infrastructural stereo camera system that includes following novel methods:

- An novel algorithm for detecting objects based on depth maps
- Simultaneous use and fusion of three different object detection algorithms
- Object localization based on stereo cameras

2 RELATED WORK

A variety of different approaches for detecting objects, mostly pedestrians, in parking garages have been developed in the past. An approach for object detection, localization and tracking in such environments based on mono cameras and a background subtraction algorithm is presented in (Ibisch et al., 2014) and (Ibisch et al., 2015). A similar method is introduced in (Einsiedler et al., 2014). Unlike these approaches, our solution uses multiple different object detection methods and thus allows the detection of dynamic as well as static objects. In (Kumar et al., 2016) an approach using a convolutional neural network (CNN) to obtain object classes is presented. The authors introduce a camera system for parking garages, that evaluates image regions in which motion was detected with a CNN for object classification. We consider the simultaneous use of a CNN and a motion detection algorithm as more advantageous. By simultaneous processing, also static objects can be detected with the CNN. An overview of multiple vehicle indoor positioning techniques including various types of sensors is given in (Einsiedler et al., 2017).

Hofmann, C., Particke, F., Hiller, M. and Thielecke, J.
Object Detection, Classification and Localization by Infrastructural Stereo Cameras.
DOI: 10.5220/0007370408080815
In *Proceedings of the 14th International Joint Conference on Computer Vision, Imaging and Computer Graphics Theory and Applications (VISIGRAPP 2019)*, pages 808-815
ISBN: 978-989-758-354-4

3 PROPOSED APPROACH

Our approach for object detection, classification and localization is based on the fusion of three algorithms. An overview is given in Figure 1. The stereo camera provides a color image, a depth map and a point cloud of the scene that is in its field of view. Following, the color image and the depth map are simultaneously processed by the three algorithms for object detection and classification. These three methods are:

- You only look once (YOLO), a convolutional neural network (CNN)
- A background subtraction algorithm (further also abbreviated BS)
- An novel algorithm for detecting salient objects in depth images (further also abbreviated SO).

Further details concerning these three object detection methods are described in the following section. The object hypotheses, i.e., the detections of each algorithm, are output in the form of bounding boxes. Subsequently, the fusion of the detection results is based on these boxes. The fusion algorithm is introduced in Section 5. Following, the resulting object hypotheses' positions in the room (3D coordinates) are determined based on the point cloud and transferred into a real-world metric coordinate system. This process is specified in Section 6. As last step, the system publishes the information about detected objects and their positions via the ROS[1] framework.

Our proposed approach is running and evaluated on a system composed of a ZED stereo camera[2] that is connected to a Jetson TX2[3] computing platform.

4 OBJECT DETECTION AND CLASSIFICATION

The use of multiple complementary object detection approaches enables our system to create a complete overview of the environment in its field of view.

Background subtraction algorithms are considered to detect moving objects in images. We apply the OpenCV[4] implementation of a background subtraction algorithm based on Gaussian Mixture Models (Zivkovic, 2004; Zivkovic and Van Der Heijden, 2006). The results of the algorithm are post-processed by applying Gaussian blur for noise reduction, morphological closing and contour extraction. Afterwards, bounding boxes enclosing the detections are created. To receive only one bounding box per object, a Non-Maximum-Suppression (NMS) algorithm is applied, similar to (Zitnick and Dollár, 2014). In contrast, we do not use the Intersection over Union (IoU) as measure for deciding whether a box is suppressed. Our approach checks if two bounding boxes intersect. In case they do, the ratio of the intersecting area to the area of the smaller box is computed. If this ratio exceeds a threshold value, the smaller bounding box is suppressed. The bigger bounding box is enlarged, so that the smaller box would be enclosed by this new bounding box. The reason for our modification of the NMS is described in more detail in Section 5, as similar principles apply to our fusion algorithm.

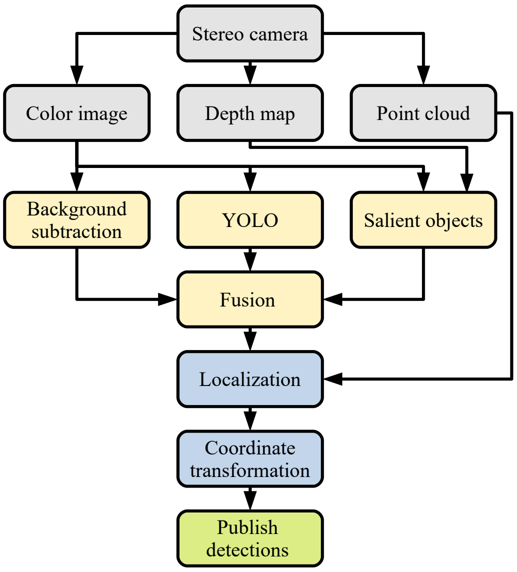

Figure 1: Processing chain of the proposed system. The stereo camera provides a color image, a depth map and a point cloud. The color image and the depth map are used for object detection and classification. The resulting detections are fused. Afterwards, the object hypotheses are localized and transformed to a real-world metric coordinate system. Finally, the object hypotheses are published.

The CNN YOLO (Redmon et al., 2016; Redmon and Farhadi, 2017) detects and classifies objects in color images. Compared to the other two algorithms, this neural network provides information about the class of the detected object. However, it is only able to detect previously trained object classes. In our system, the tiny version of YOLOv2 (Tiny YOLO)[5] is used, as the computation time per image is significantly smaller on the Jetson TX2 compared to the full version. We use pretrained weights based on the COCO[6] dataset.

[1] http://www.ros.org/

[2] https://www.stereolabs.com

[3] https://www.nvidia.com

[4] https://opencv.org/

[5] https://pjreddie.com/darknet/yolov2/

[6] cocodataset.org

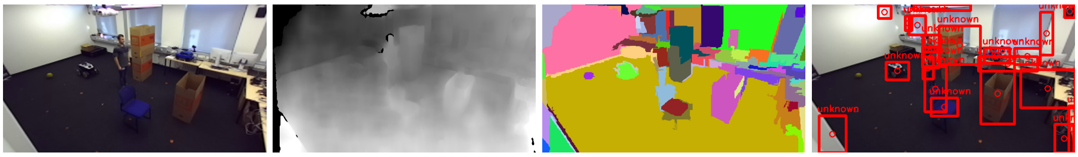

Color image Depth map Segmentation Detection results

Figure 2: Example application of the SO algorithm. The resulting segmentation based on the color image (left) and the depth map (middle left) is depicted in the middle right with a different color for each segment. The color image with bounding boxes enclosing detected salient objects is depicted on the right.

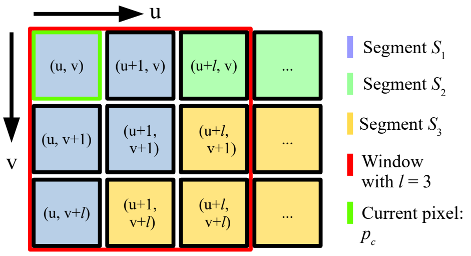

Figure 3: Example search window of the SO algorithm.

The third algorithm is a novel approach inspired by salient object detection algorithms presented in (Ju et al., 2014) and (Feng et al., 2016). The key point of salient object detection algorithms is the comparison whether some image region is closer to the camera than a certain environment around. Those algorithms are mainly designed and evaluated for one salient object in the picture, so that we developed a new approach to detect multiple salient objects. Our approach builds on the image segmentation algorithm presented in (Felzenszwalb and Huttenlocher, 2004). The color image as well as the depth map are used in the segmentation algorithm to divide the depth map into I segments (cf. Figure 2). After the segmentation, for each pixel p at the image coordinates (u, v), its depth d_p and the segment S_i it belongs to is known, with $i \in I$. We define the property $F(S_i)$, that describes a measure whether the segment S_i depicts a foreground object or background. First, the pixel in the top left corner of the image is chosen as a current pixel p_c. Based on this current pixel p_c, a quadratic search window W with an edge length of l pixels is created. An example search window is depicted in Figure 3. For each pixel in this window is checked, if it belongs to the same segment as the current pixel p_c. The pixel with the maximal distance to the camera p_w that does not belong to the current pixel's segment S_i is selected, since it is the most probable candidate to represent the background. The depth difference $m(p_c, p_w)$ between the current pixel p_c and the selected pixel p_w is calculated by

$$m(p_c, p_w) = d_{p_c} - d_{p_w} \,. \tag{1}$$

The result of this subtraction is positive if the current pixel p_c is closer to the camera, i.e., depicts more probable a foreground object. It is negative if the selected pixel p_w is nearer to the camera, i.e., the current pixel p_c belongs more probable to the background. The algorithm processes every pixel p in the image as current pixel p_c. Accordingly, we move the search window W with a stride of one pixel. If all pixels inside the window W belong to the same segment S_i, no action is performed. In case a search window W exceeds the image dimensions, only the available pixels are included to the window. To decide whether a segment S_i represents a foreground object, we calculate the property $F(S_i)$ as follows

$$F(S_i) = \sum_{p_c \in S_i} m(p_c, p_w) + \sum_{p_w \in S_i} m(p_c, p_w) \,. \tag{2}$$

All results of depth comparisons $m(p_c, p_w)$ incorporating pixels of the segment S_i, either as actual pixel p_c or as pixel with maximal distance inside the search window p_w, are summed up. Since small segments provide fewer comparisons with other segments, we normalize $F(S_i)$, so that all segments S are comparable. For normalizing, $F(S_i)$ is divided by the number N_i of comparison results $m(p_c, p_w)$ which were added to $F(S_i)$ follows

$$F_N(S_i) = \frac{F(S_i)}{N_i} \,. \tag{3}$$

The decision whether a segment S_i depicts a foreground object is defined as

$$S_i = \begin{cases} \text{foreground object} & F_N(S_i) > F_{th} \\ \text{background} & F_N(S_i) \leq F_{th} \,, \end{cases} \tag{4}$$

where F_{th} is a threshold value. Bounding boxes are created enclosing the segments which represent foreground objects. Our NMS algorithm is applied to these bounding boxes.

The SO algorithm requires a relative long processing time of about 0.33 s per image (BS: 0.08 s, YOLO: 0.13 s). To increase the average measurement rate, we apply the SO algorithm periodically (3 s), while the other algorithms evaluate each image. This periodical evaluation brings no further disadvantages. Static objects of special interest can be trained for being detected by YOLO and moving objects are detected by the BS algorithm with a high detection rate.

5 FUSION OF THE OBJECT HYPOTHESES

To combine the detection results of the three different algorithms, we propose a fusion algorithm based on bounding boxes. We make the reasonable assumption that if the algorithms detect the same object and output their detection as bounding boxes, these boxes intersect largely.

The fusion algorithm checks in a first step if the bounding boxes from any two different algorithms overlap. In the case that two boxes B_k and B_l intersect, the ratio R between the area of intersection $B_k \cap B_l$ and the area of the smaller one of the two boxes is computed by

$$R = \begin{cases} \frac{\text{area}(B_k \cap B_l)}{\text{area}(B_k)} & \text{if} \quad \text{area}(B_k) \leq \text{area}(B_l) \\ \\ \frac{\text{area}(B_k \cap B_l)}{\text{area}(B_l)} & \text{if} \quad \text{area}(B_k) > \text{area}(B_l)\,. \end{cases} \tag{5}$$

This ratio R allows the fusion of boxes also if the smaller box is completely enclosed by the other box and of relatively small size compared to it. An example is a standing person that turns its head. The background subtraction detects only the movement of the head, whereas YOLO and SO detect the whole person. The fusion would not be performed, if the common IoU metric is used. However, if the introduced ratio R exceeds a certain threshold value, the boxes are fused and a new bounding box which encloses the two original boxes is created. In this process, also the information of the detected objects are fused, i.e., the class and the dynamic state. The results for the different possible pairings are shown in Table 1. In the case, that the background subtraction detects an object, this object must be moving, i.e., a dynamic object. If an object is not detected by the background subtraction, whereas it is detected by another detection method, this object is considered as static. In this first step, it is possible, that one box is fused multiple times with other boxes. The new bounding boxes created by the fusion process are not used for further fusion at this stage.

In the second step of the algorithm only the fusion results of step one and previously not fused bounding boxes are still of interest. The boxes that were not fused before are passed through as final detection results. It is possible, that there are multiple object hypotheses from step one for a single real object (cf. Figure 4). Consequently, the fusion results from step one are fused again according to the bounding box fusion procedure described before. If now two boxes with different classes from YOLO are to be fused, the fusion result inherits the class with the higher confidence value provided by YOLO.

As aforementioned, the algorithm is designed to fuse the results of two object detection algorithms. However, our system works with three approaches. The fusion of three approaches is performed by first fusing two of them. The fusion results as well as the not fused detections are then separately fused with the results of the third algorithm.

Table 1: Possible information fusion outcomes. The "+" shows, that the SO algorithms provides no new information, but increases the evidence for an object being present.

BS	YOLO	SO	Object hypothesis
✓	-	-	dynamic unknown object
-	✓	-	static classified object
-	-	✓	static unknown object
✓	✓	-	dynamic classified object
✓	-	✓	dynamic unknown object +
-	✓	✓	static classified object +
✓	✓	✓	dynamic classified object +

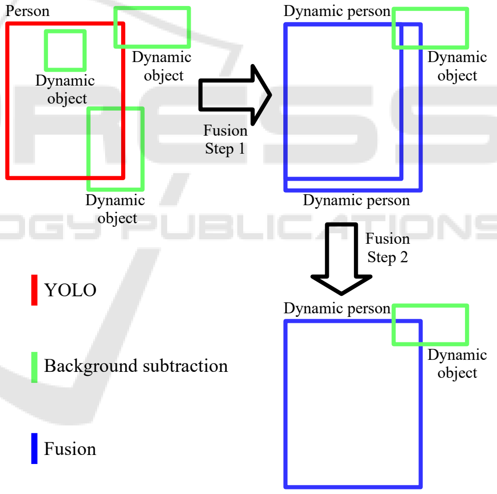

Figure 4: Example for the bounding box fusion algorithm. A person and three moving objects are detected. In the first fusion step, two moving objects are fused with the detected person. The third moving object intersects not sufficient with another bounding box to be fused. In the second fusion step, the two boxes describing a dynamic person are fused, as they largely intersect.

6 OBJECT LOCALIZATION

The localization in the real world of previously in the image detected objects is performed by using the point cloud. The point cloud is computed with the two images of the stereo camera, as described for example in (Hartley and Zisserman, 2003).

Since real world objects often have no rectangular shape and the detection results can be faulty, the bounding boxes partly enclose the background in many cases. This leads to a difficult localization of the whole foreground object, as a highly accurate segmentation would be necessary to distinguish between object and background. An approach for such high accuracy segmentations based on bounding boxes is presented in (Lempitsky et al., 2009). The crucial point is, that up to now the computing power of small platforms (like the Jetson TX2) is not sufficient to solve this task in an acceptable time. As a consequence, our localization approach is based on the 3D position of the pixels in the center of the bounding box. It is very likely, that in the center of the box the detected object is present. Based on this assumption, the 3D coordinates corresponding to the pixels in the center of the bounding box are extracted from the point cloud. We extract 144 points corresponding to the pixels around the center, according to the size of the smallest object to be detected. The median for the *x*-, *y*-, *z*- position is calculated to deal with possible outliers.

Since the coordinates of the point cloud are expressed in the camera coordinate system (cf. Figure 5), we transform the position of the detected objects in a real-world metric coordinate system. Therefore the translation and rotation between this two coordinate systems is necessary. By once placing a checkerboard in the field of view of the camera, it is possible to receive the extrinsic parameters. These parameters describe the transformation between the camera coordinate system and a real-world metric coordinate system that is based on the checkerboard pattern (Zhang, 2000; Kaehler and Bradski, 2016).

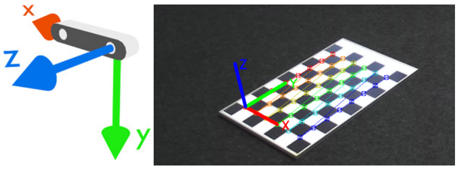

Figure 5: Camera coordinate system (left, https://www.stereolabs.com) and coordinate system defined by the checkerboard pattern (right)

After this step, the following information about detected objects are published:

- Time of the measurement
- Class of the detected object, which can also be unknown, if no class is provided by YOLO
- Dynamic state of the object (static or dynamic)
- 3D-position in the real world metric coordinate system

7 EVALUATION ON REAL WORLD DATA

For the evaluation of our proposed system, we use a test scenario consisting of different objects. These objects are a chair, a sports ball, a robot and some cardboard boxes, all placed on defined positions. This setup is shown in Figure 6. Additionally to these objects, a person is walking through the scenario and rests for several seconds at two specific positions (see Figure 7). The person enters the measurement setup at the coordinates (3.5, 1), walks to (0, -1), turns right and rests at (0, 2) (”Person A”) for a short time. Then the person moves according to the trajectory to the position ”Person B” and rests again. From there, the person moves to (1, -1), turns left and returns to the starting position.

We evaluate the systems for two different camera positions, as pictured in Figure 6. For evaluating the three algorithms and the fusion, we use 150 images of the measurement setup including the person captured from each camera position. For investigating the whole system, we saved the detection, classification and localization results in another measurement run.

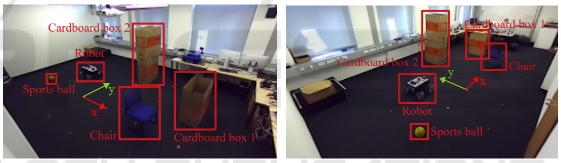

Camera position 1 Camera position 2

Figure 6: Images of the measurement setup with the placed static objects seen from the two camera positions.

In the evaluation setup, the walking person is the only dynamic object, hence the only detectable object for the BS. The training dataset of YOLO includes the classes chair, sports ball and person, so these three objects in the test setup are to be detected and classified by the CNN. The person can be detected by the CNN when moving, but also when resting. The algorithm for detecting salient objects is able to detect all the objects in the our setup, including the robot and the cardboard boxes.

To evaluate the algorithms and the fusion algorithm, we use the IoU metric for evaluating bounding boxes described in (Everingham et al., 2010). First, for all images the true bounding boxes and classes were annotated by hand. Afterwards, a program checks if a bounding box from an algorithm or the fusion has an IoU with a true bounding box $\geqq 0.5$. If so, the box is considered as correct detection. In the case that multiple boxes have an IoU $\geqq 0.5$ with the same true box, only the box with the greatest IoU is considered as correct. The other ones are considered as false detections, similar to bounding boxes that have an IoU < 0.5 or no intersection with a true box. Missed detections are counted in case that an object is not detected. We define the detection ratio as correct detections over possible detections. If a detection is correct, it is checked if also the classification is right.

In Table 2 the evaluation results of background subtraction, YOLO and the their fusion only for detecting and classifying the person (walking and resting) are presented. With the camera at position one, the background subtraction works quite well at any time, as the moving person is always detected. YOLO detects the person walking only occasional and never the person resting. If YOLO detects the person, the classification is always correct. The number of detections made by YOLO is influenced by the minimal confidence threshold for outputs (see also (Redmon et al., 2016)), which we selected 0.5. By selecting this value, we have a balance between too many false detections and too few correct detections. The fact that YOLO does not detect the resting person leads to the effect that with the fusion the detection rate is not increased. The absolute number of correct classifications increases from 21 to 27 due to the fusion. By the fusion, the bounding box size of too small boxes from YOLO is corrected based on the boxes from the background subtraction. The wrong detections of the background subtraction and subsequent of the fusion are caused by shadows, which are generated by the person. The false detections from YOLO are those too small bounding boxes, that are eliminated by the fusion algorithm. At camera position two, the detection rate increases by using the fusion as YOLO can also detect the person resting at certain instances (cf. Figure 7). Similar to camera position one, the effect concerning increased absolute correct classifications is visible. The number of false detections is high compared to camera at position one. This high number is on the one hand caused by the shadows, as already described. On the other hand, the walking person is relatively far away from the camera (about 8 meters) at its starting position and endpoint. At these distances the background subtraction algorithm creates too big bounding boxes. This results in a false and a missed detection. YOLO outputs 17 false detections, as for the person resting at position B two bounding boxes are created (see Figure 7). Accordingly, one of the two bounding boxes is considered as false.

Summed up, this first evaluation proofs that by applying our fusion approach, the detection of the person improves compared to using only the CNN or the background subtraction. Furthermore, the system can classify the person additionally in some images, what can be used in a future tracking algorithm to classify objects, also when no detection is provided by the CNN.

Table 2: Evaluation of the BS algorithm, YOLO and their fusion for the person.

Camera Position 1			
Method	BS	YOLO	Fusion
Possible detections	118	118	118
Correct detections	95	21	95
Detection ratio	0.81	0.18	0.81
Correct classifictations	-	21	27
Missed dections	23	97	23
False detections	9	6	9

Camera Position 2			
Method	BS	YOLO	Fusion
Possible detections	139	139	139
Correct detections	96	53	114
Detection ratio	0.69	0.38	0.82
Correct classifictations	-	53	61
Missed dections	43	86	25
False detections	31	17	43

Table 3: Evaluation of the SO algorithm and the fusion of all three algorithms for all objects in the measurement setup.

Camera	Position 1		Position 2	
Method	SO	Fusion	SO	Fusion
Possible detections	832	832	860	860
Correct detections	303	397	352	454
Detection ratio	0.36	0.48	0.41	0.53
Missed dections	529	435	508	406
False detections	495	383	412	342

In Table 3 the results of the SO algorithm and the fusion of all three algorithms are presented. For this evaluation, the SO algorithm was not applied periodically but to every image. The number of total possible detections increases, as now all objects in the measurement setup are detectable for our system. Since the SO algorithm detects objects in the whole image (see Figure 2), we adopted the evaluation metric for this algorithm, so that only the placed test objects are included in the evaluation. Only bounding boxes from SO that have an IoU with a true box > 0.1 are considered. By using this threshold, only bounding boxes that show a sufficient cue for being a detection (also false) of the placed object are evaluated. The detection ratio of SO is only 0.36. Moreover, there is a great number of false detections. These numbers arise from too small bounding boxes for detected objects output by the SO algorithm. Consequently, the IoU with a true box is < 0.5 and thus a false detection. Those false box dimensions are caused by the segmentation, as the segments often do not fit to the real object shapes. Furthermore, objects that were relatively far away from the camera were not detected well, as also obvious in Figure 7. The reason therefore is, that with increasing distance the quality of the depth estimation declines. Comparing the results of the SO algorithm with those of the fusion, the improvements by the fusion are clearly visible.

In Figure 7, the detection, classification and localization results from both camera positions are depicted. It is to note, that in this figure all detections of the system are presented, also detections that were considered as false in the evaluation before. The results are depicted in the *x*-*y*-plane of the coordinate system defined by the checkerboard pattern. For clarity we have split the results showing detected dynamic objects (top) and detected static objects (bottom).

The top maps of Figure 7 depict the detected dynamic objects, in the evaluation scenario the walking person. Additionally, the ground truth of the person's trajectory is shown. The moving person is detected and localized on the whole trajectory. However, there are many detections of the person as unknown dynamic object (BS) and some as dynamic person (fusion). These results are consistent with the evaluation before. The errors in the localization are explainable by:

- Faulty 3D coordinates of the point cloud
- Errors in the transformation between the coordinate systems
- The detected object is not present in the center of the bounding box, so that a point in the background is localized.

Since we achieved a mean reprojection error by averaging the reprojection errors of all checkerboard corners of 0.14 pixels for camera position one and 0.25 pixels for camera position two, we infer that the transformation between the coordinate systems has only a small impact on the localization error. Moreover, the real person has dimensions larger than the line used as ground truth. A small deviation of the person's localization from this line is accordingly not surprising. Averaging the minimal euclidean distance to the true trajectory for all measurements, we achieve a mean error of 0.1 meters for the camera at position one and of 0.13 meters for the camera at position two.

Considering the static objects (Figure 7 bottom), the system only detects those objects that are relatively near to the camera. Furthermore, the number of detections of cardboard boxes is small compared to number of chair detections. The SO algorithm detects the cardboard boxes only periodically (3 s), whereas YOLO is able to detect the chair approximately in every obtained measurement. This effect is also visible at camera position two. The localization error of the detections of the chair, sports ball and robot is very small, and different measurements are localized close

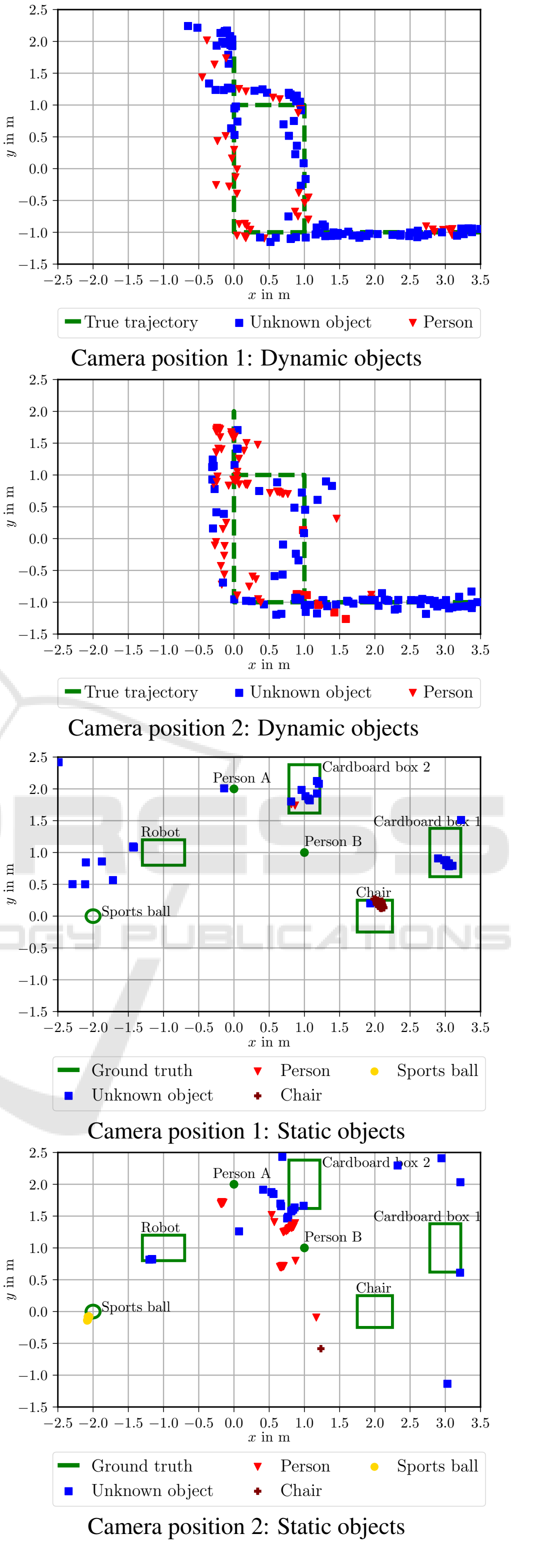

Camera position 1: Dynamic objects

Camera position 2: Dynamic objects

Camera position 1: Static objects

Camera position 2: Static objects

Figure 7: Localization results obtained with our system and ground truth depicted in the *x*-*y*-plane of the checkerboard coordinate system.

together. The bounding boxes for these objects were always chosen very similarly, which leads to this closely spaced localization pattern. In contrast, the bounding boxes for the cardboard boxes often had different sizes. This results in the wider spread of the localizations. In the bottom maps of Figure 7 also some false measurements are present. These measurements are mostly caused by the SO algorithm, due to false localizations of other objects in the room. We reach an average detection rate of approximately 7.5 Hz, which is sufficient for a real time application.

8 CONCLUSION AND FUTURE WORK

In this contribution, we presented an infrastructural stereo camera system for real-time object detection, classification and localization. By using three different complementary approaches for object detection, the system has the ability to detect almost every object in its field of view. With our proposed fusion algorithm for bounding boxes we improved the detection and classification results, as presented in the evaluation. The localization approach based on the stereo camera shows satisfying results. However, further research concerning the localization of the whole object, not only a point, is of high interest. In the future, we plan to improve the detections by training the CNN with images captured by the system. Furthermore, improvements concerning the algorithm for salient object detection are planned. Additionally, we will expand the system by a tracking algorithm.

REFERENCES

Einsiedler, J., Becker, D., and Radusch, I. (2014). External visual positioning system for enclosed carparks. In *Positioning, Navigation and Communication (WPNC), 2014 11th Workshop on*, pages 1–6. IEEE.

Einsiedler, J., Radusch, I., and Wolter, K. (2017). Vehicle indoor positioning: A survey. In *Positioning, Navigation and Communications (WPNC), 2017 14th Workshop on*, pages 1–6. IEEE.

Everingham, M., Van Gool, L., Williams, C. K., Winn, J., and Zisserman, A. (2010). The pascal visual object classes (voc) challenge. *International journal of computer vision*, 88(2):303–338.

Felzenszwalb, P. F. and Huttenlocher, D. P. (2004). Efficient graph-based image segmentation. *International journal of computer vision*, 59(2):167–181.

Feng, D., Barnes, N., You, S., and McCarthy, C. (2016). Local background enclosure for rgb-d salient object detection. In *Proceedings of the IEEE Conference on Computer Vision and Pattern Recognition*, pages 2343–2350.

Hartley, R. and Zisserman, A. (2003). *Multiple view geometry in computer vision*. Cambridge university press.

Ibisch, A., Houben, S., Michael, M., Kesten, R., and Schuller, F. (2015). Arbitrary object localization and tracking via multiple-camera surveillance system embedded in a parking garage. In *Video Surveillance and Transportation Imaging Applications 2015*, volume 9407, page 94070G. International Society for Optics and Photonics.

Ibisch, A., Houben, S., Schlipsing, M., Kesten, R., Reimche, P., Schuller, F., and Altinger, H. (2014). Towards highly automated driving in a parking garage: General object localization and tracking using an environment-embedded camera system. In *Intelligent Vehicles Symposium Proceedings, 2014 IEEE*, pages 426–431. IEEE.

Ju, R., Ge, L., Geng, W., Ren, T., and Wu, G. (2014). Depth saliency based on anisotropic center-surround difference. In *Image Processing (ICIP), 2014 IEEE International Conference on*, pages 1115–1119. IEEE.

Kaehler, A. and Bradski, G. (2016). *Learning OpenCV 3: computer vision in C++ with the OpenCV library*. O'Reilly Media, Inc.

Kumar, A. K. T. R., Schäufele, B., Becker, D., Sawade, O., and Radusch, I. (2016). Indoor localization of vehicles using deep learning. In *World of Wireless, Mobile and Multimedia Networks (WoWMoM), 2016 IEEE 17th International Symposium on A*, pages 1–6. IEEE.

Lempitsky, V. S., Kohli, P., Rother, C., and Sharp, T. (2009). Image segmentation with a bounding box prior. In *ICCV*, pages 277–284. Citeseer.

Redmon, J., Divvala, S., Girshick, R., and Farhadi, A. (2016). You only look once: Unified, real-time object detection. In *Proceedings of the IEEE conference on computer vision and pattern recognition*, pages 779–788.

Redmon, J. and Farhadi, A. (2017). Yolo9000: better, faster, stronger. *arXiv preprint*.

Zhang, Z. (2000). A flexible new technique for camera calibration. *IEEE Transactions on pattern analysis and machine intelligence*, 22(11):1330–1334.

Zitnick, C. L. and Dollár, P. (2014). Edge boxes: Locating object proposals from edges. In *European conference on computer vision*, pages 391–405. Springer.

Zivkovic, Z. (2004). Improved adaptive gaussian mixture model for background subtraction. In *Pattern Recognition, 2004. ICPR 2004. Proceedings of the 17th International Conference on*, volume 2, pages 28–31. IEEE.

Zivkovic, Z. and Van Der Heijden, F. (2006). Efficient adaptive density estimation per image pixel for the task of background subtraction. *Pattern recognition letters*, 27(7):773–780.